

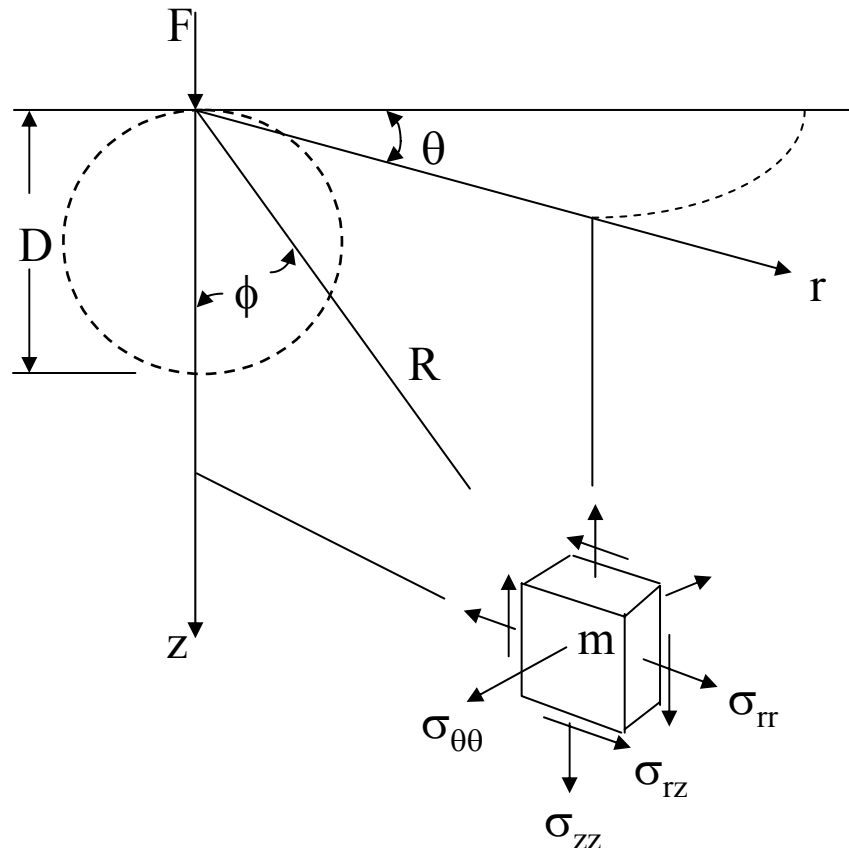
Chapter 4

Response of Materials to Surface Traction

Response of Materials

- 1. Deformation of the surface and subsurface**
- 2. Fracture of Solids**

Point Force Applied to a Semi-Infinite Elastic Solid



Point force P is applied at the origin of the cylindrical coordinate system(r, θ, z).

Point Force Applied to a Semi-Infinite Elastic Solid (Boussinesq solution)

$$\sigma_{rr} = \frac{P}{2\pi} \left[(1 - 2\nu) \frac{1}{r^2} - \frac{z}{r^2(r^2 + z^2)^{1/2}} - \frac{3r^2 z}{(r^2 + z^2)^{5/2}} \right]$$

$$\sigma_{zz} = -\frac{3P}{2\pi} \frac{z^3}{(r^2 + z^2)^{5/2}}$$

$$\sigma_{\theta\theta} = \frac{(1 - 2\nu)P}{2\pi} \left[-\frac{1}{r^2} + \frac{z}{r^2(r^2 + z^2)^{1/2}} + \frac{z}{(r^2 + z^2)^{3/2}} \right]$$

$$\sigma_{rz} = -\frac{3P}{2\pi} \frac{rz^2}{(r^2 + z^2)^{5/2}}$$

Point Force Applied to a Semi-Infinite Elastic Solid -- Resultant stress on face m

$$\sigma^R = \sigma_{zz}^2 + \sigma_{rz}^2 = \frac{3P}{2\pi} \frac{z^2}{(r^2+z^2)^2} = \frac{3P}{2\pi} \frac{\cos^2 \phi}{(r^2+z^2)^2} = \frac{3P}{2\pi D^2}$$

where

D is the diameter of the sphere passing through the point of application of the force.

Point Force Applied to a Semi-Infinite Elastic Solid

$$\begin{aligned} u &= \frac{(1 - 2\nu)(1 + \nu)P}{2\pi Er} \left[\frac{z}{(r^2 + z^2)^{1/2}} - 1 + \frac{r^2 z}{(1 - 2\nu)(r^2 + z^2)^{3/2}} \right] \\ v &= 0 \\ w &= \frac{P}{2\pi E} \left[\frac{(1 + \nu) z^2}{(r^2 + z^2)^{3/2}} + \frac{2(1 - \nu^2)}{(r^2 + z^2)^{1/2}} \right] \end{aligned} \quad (4.3)$$

At $z = 0$, the radial and the vertical components of displacement become

$$\begin{aligned} u &= -\frac{(1 - 2\nu)(1 + \nu)P}{2\pi Er} \\ w &= \frac{(1 - \nu^2)P}{\pi Er} \end{aligned} \quad (4.4)$$

According to Eq. (4.4), the radial and vertical displacements at the surface decrease inversely with distance from the origin.

Trajectory of Principal stresses due to a Point Force

Diagram removed for copyright reasons.

See Figure 4.2 in [Suh 1986]: Suh, N. P. *Tribophysics*. Englewood Cliffs NJ: Prentice-Hall, 1986. ISBN: 0139309837.

Contour of Principal Normal Stresses ($\nu=0.25$)

Diagram removed for copyright reasons.

See Figure 4.3 in [Suh 1986]: Suh, N. P. *Tribophysics*. Englewood Cliffs NJ: Prentice-Hall, 1986. ISBN: 0139309837.

Angular Variation of Principal Stress Components in Boussinesq Field ($\nu=0.25$)

Diagram removed for copyright reasons.

See Figure 4.4 in [Suh 1986]: Suh, N. P. *Tribophysics*. Englewood Cliffs NJ: Prentice-Hall, 1986. ISBN: 0139309837.

Hertzian Contact

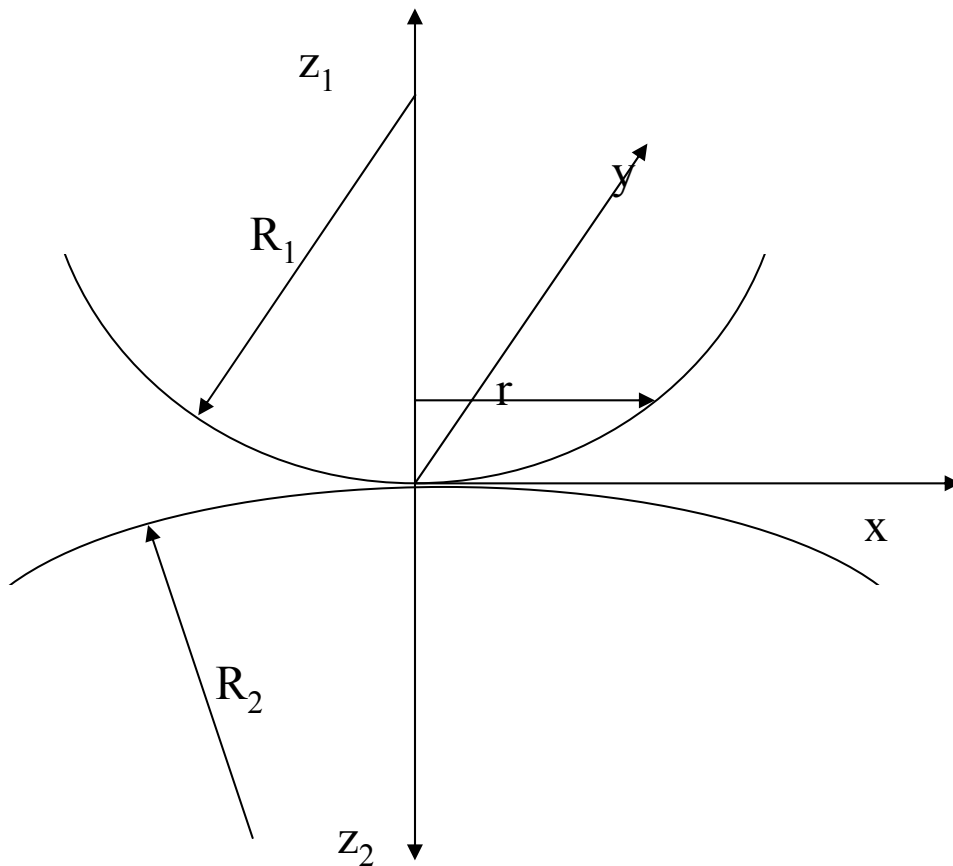


Figure 4.5 Two spherical bodies in contact.

At zero load the contact occurs at a point $x = y = z_1 = z_2 = 0$. ¹⁰

Hertzian Stress due to Spherical Indenters

(Normal Stress Distribution)

$$(\sigma_{zz})_{z=0} = -p = -p_0 \frac{(a^2 - r^2)^{1/2}}{a}$$

Hertzian Stress due to Spherical Indenters (Normal Stress Distribution)

$$a = \left[\frac{3P}{16} \frac{k_1 + k_2}{\rho_1 + \rho_2} \right]^{1/3} = \left[\frac{3P}{4} \frac{(k_1 + k_2) R_1 R_2}{R_1 + R_2} \right]^{1/3}$$

$$p_0 = \frac{3P}{2\pi a^2}$$

where

$$k_i = \frac{1 - \nu_i^2}{E_i} \quad i = 1 \text{ or } 2$$

$$\rho_i = \frac{1}{R_i} = \text{curvature of the sphere } i$$

Location of the Max. Radial Stress

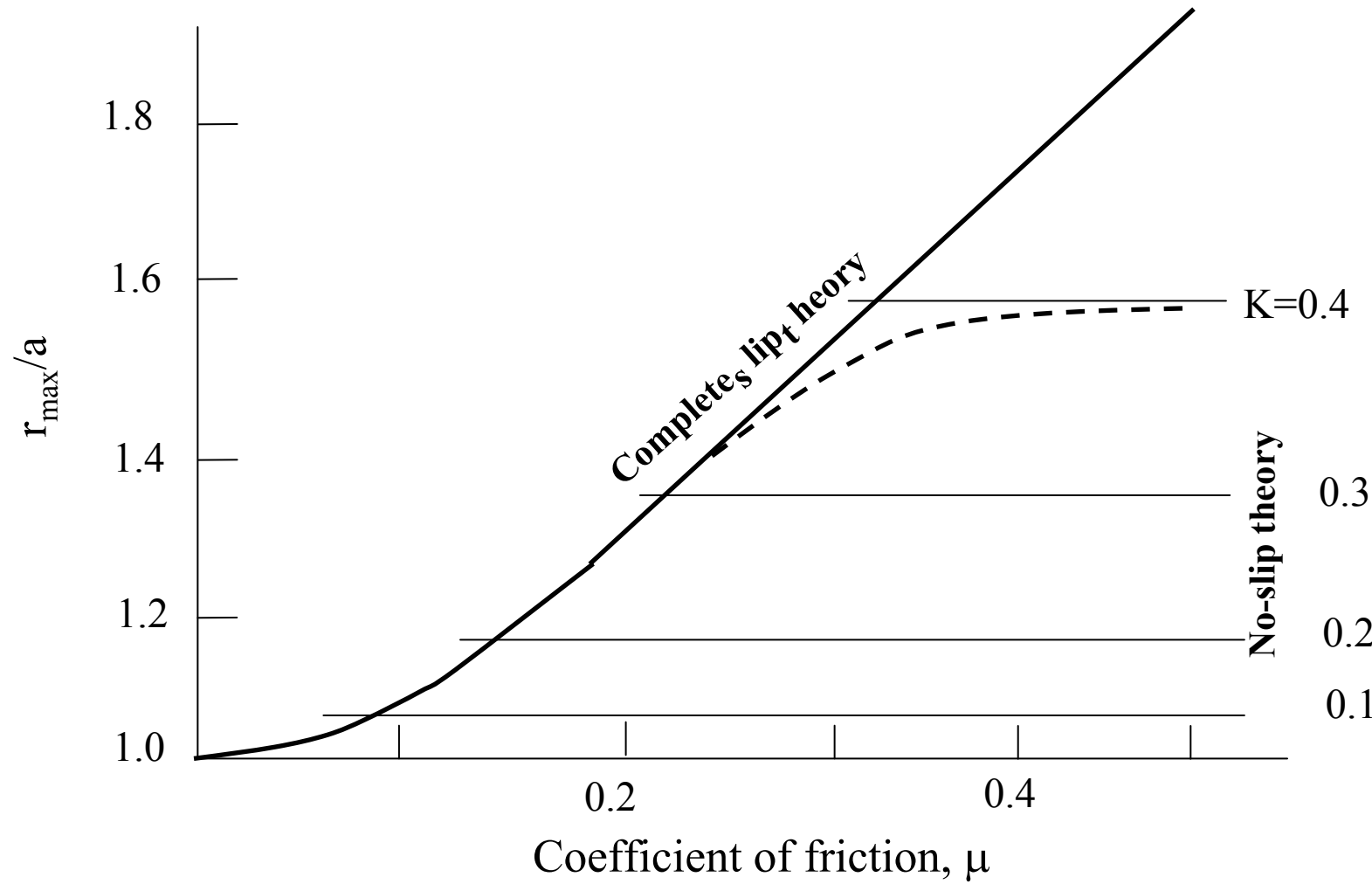


Figure 4.6 Position of the maximum radial tensile stress

Stress Field due to Line Load

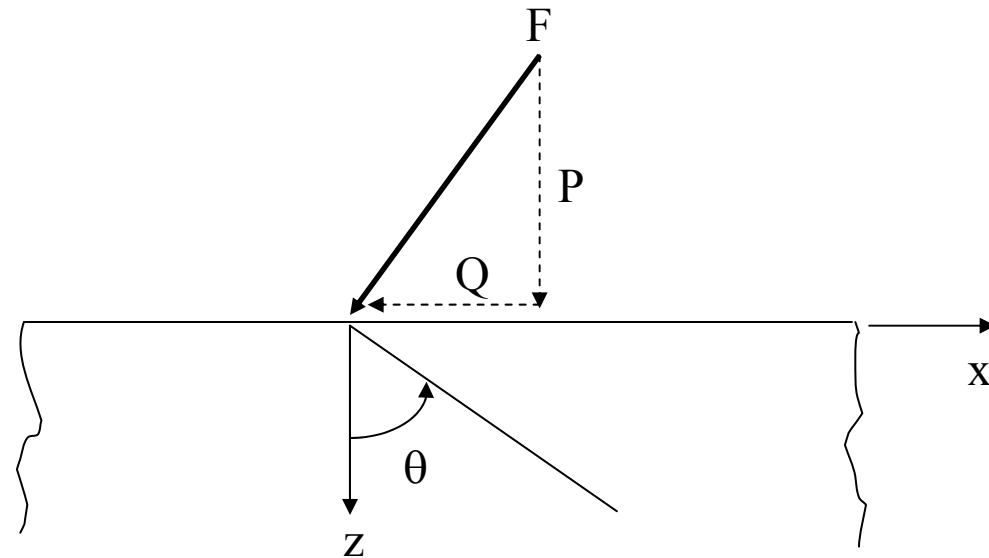


Figure 4.7 Semi-infinite elastic solid loaded by a concentrated load

Stress Field due to Line Load

$$\begin{aligned}\sigma_{xx} &= -\frac{2P}{\pi z} \cos^2 \theta \sin^2 \theta + \frac{2Q}{\pi z} \sin^3 \theta \cos \theta = \Lambda \sin^2 \theta \\ \sigma_{zz} &= -\frac{2P}{\pi z} \cos^4 \theta + \frac{2Q}{\pi z} \cos^3 \theta \sin \theta = \Lambda \cos^2 \theta \\ \sigma_{xz} &= -\frac{2P}{\pi z} \sin \theta \cos^3 \theta + \frac{2Q}{\pi z} \cos^2 \theta \sin^2 \theta = \Lambda \sin \theta \cos \theta\end{aligned}\tag{4.9}$$

where the angle θ and the function Λ are given by

$$\theta = \cos^{-1} \frac{z}{(x^2 + z^2)^{1/2}} \quad \Lambda = \frac{2}{\pi z} (-P \cos^2 \theta + Q \sin \theta \cos \theta)$$

Semi-infinite elastic solid loaded by a elliptical distributed load

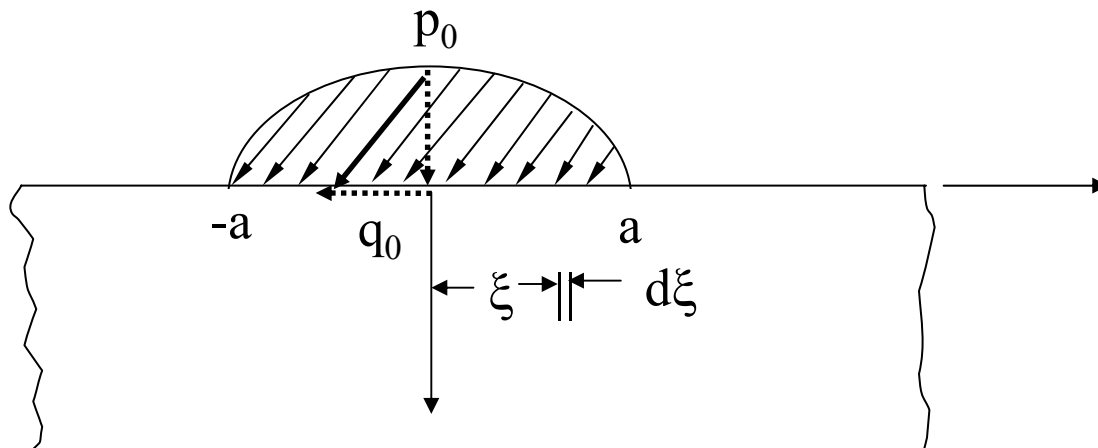


Figure 4.8 Semi-infinite elastic solid loaded by a elliptical distributed load. The maximum normal and tangential stresses are p_0 and q_0 , respectively.

Semi-infinite elastic solid loaded by a elliptical distributed load

$$\sigma_{zz} = \begin{cases} 0 & \text{for } |x| > a \\ -p_0 \left(1 - \frac{x^2}{a^2} \right)^{1/2} & \text{for } |x| \leq a \end{cases}$$

$$\sigma_{xz} = \begin{cases} 0 & \text{for } |x| > a \\ q_0 \left(1 - \frac{x^2}{a^2} \right)^{1/2} & \text{for } |x| \leq a \end{cases}$$

The maximum normal and tangential stresses are p_0 and q_0 , respectively.

Semi-infinite elastic solid loaded by a elliptical distributed load

$$\begin{aligned}
 \sigma_{xx} &= \frac{2q_0}{\pi za} \int_{-a}^a (a^2 - \xi^2)^{1/2} \frac{(x - \xi)^3 z}{[z^2 + (x - \xi)^2]^2} d\xi \\
 &\quad - \frac{2P_0}{\pi az} \int_{-a}^a (a^2 - \xi^2)^{1/2} \frac{z^2(x - \xi)^2}{[z^2 + (x - \xi)^2]^2} d\xi \\
 \sigma_{zz} &= \frac{2q_0}{\pi az} \int_{-a}^a (a^2 - \xi^2)^{1/2} \frac{(x - \xi)z^3}{[z^2 + (x - \xi)^2]^2} d\xi \\
 &\quad - \frac{2P_0}{\pi az} \int_{-a}^a (a^2 - \xi^2)^{1/2} \frac{z^4}{[z^2 + (x - \xi)^2]^2} d\xi \\
 \sigma_{xz} &= \frac{2q_0}{\pi az} \int_{-a}^a (a^2 - \xi^2)^{1/2} \frac{(x - \xi)^2 z^2}{[z^2 + (x - \xi)^2]^2} d\xi \\
 &\quad - \frac{2P_0}{\pi az} \int_{-a}^a (a^2 - \xi^2)^{1/2} \frac{z^3(x - \xi)}{[z^2 + (x - \xi)^2]^2} d\xi
 \end{aligned} \tag{4.13}$$

18

The maximum normal and tangential stresses are p_0 and q_0 , respectively.

Semi-infinite elastic solid loaded by a elliptical distributed load

$$\begin{aligned}
 \sigma_{xx} &= \frac{q_0}{\pi} \left[(2x^2 - 2a^2 - 3z^2)\psi + 2\pi \frac{x}{a} + 2(a^2 - x^2 - z^2) \frac{x}{a} \bar{\psi} \right] \\
 &\quad - \frac{P_0}{\pi} z \left(\frac{a^2 + 2x^2 + 2z^2}{a} \bar{\psi} - \frac{2}{a} - 3x\psi \right) \\
 \sigma_{zz} &= \frac{q_0}{\pi} z^2 \psi - \frac{P_0}{\pi} z (a\bar{\psi} - x\psi) \\
 \sigma_{xz} &= \frac{q_0}{\pi} \left[(a^2 + 2x^2 + 2z^2) \frac{z}{a} \bar{\psi} - 2\pi \frac{z}{a} - 3xz\psi \right] - \frac{P_0}{\pi} z^2 \psi
 \end{aligned} \tag{4.14}$$

in which

$$\psi \equiv \frac{\pi}{k_1} \frac{1 - (k_2/k_1)^{1/2}}{(k_2/k_1)^{1/2} \{ 2(k_2/k_1)^{1/2} + [(k_1 + k_2 - 4a^2)/k_1] \}^{1/2}} \tag{4.15}$$

$$\bar{\psi} \equiv \frac{\pi}{k_1} \frac{1 + \left(\frac{k_2}{k_1}\right)^{1/2}}{(k_2/k_1)^{1/2} \{ 2(k_2/k_1)^{1/2} + [(k_1 + k_2 - 4a^2)/k_1] \}^{1/2}}$$

$$k_1 \equiv (a + x)^2 + z^2$$

$$k_2 \equiv (a - x)^2 + z^2$$

Semi-infinite elastic solid loaded by a elliptical distributed load

$$\begin{aligned}
 \sigma_{xx} &= \frac{q_0}{\pi} \left[(2x^2 - 2a^2 - 3z^2)\psi + 2\pi \frac{x}{a} + 2(a^2 - x^2 - z^2) \frac{x}{a} \bar{\psi} \right] \\
 &\quad - \frac{P_0}{\pi} z \left(\frac{a^2 + 2x^2 + 2z^2}{a} \bar{\psi} - \frac{2}{a} - 3x\psi \right) \\
 \sigma_{zz} &= \frac{q_0}{\pi} z^2 \psi - \frac{P_0}{\pi} z (a\bar{\psi} - x\psi) \\
 \sigma_{xz} &= \frac{q_0}{\pi} \left[(a^2 + 2x^2 + 2z^2) \frac{z}{a} \bar{\psi} - 2\pi \frac{z}{a} - 3xz\psi \right] - \frac{P_0}{\pi} z^2 \psi
 \end{aligned} \tag{4.14}$$

in which

$$\begin{aligned}
 \psi &\equiv \frac{\pi}{k_1} \frac{1 - (k_2/k_1)^{1/2}}{(k_2/k_1)^{1/2} \{2(k_2/k_1)^{1/2} + [(k_1 + k_2 - 4a^2)/k_1]\}^{1/2}} \\
 &\quad 1 + \left(\frac{k_2}{k_1} \right)^{1/2}
 \end{aligned} \tag{4.15}$$

$$\bar{\psi} \equiv \frac{\pi}{k_1} \frac{1}{(k_2/k_1)^{1/2} \{2(k_2/k_1)^{1/2} + [(k_1 + k_2 - 4a^2)/k_1]\}^{1/2}}$$

$$k_1 \equiv (a + x)^2 + z^2$$

$$k_2 \equiv (a - x)^2 + z^2$$

Semi-infinite elastic solid loaded by a elliptical distributed load

$$\sigma_{xx} = \begin{cases} 2q_0 \left[\frac{x}{a} - \left(\frac{x^2}{a^2} - 1 \right)^{1/2} \right] & \text{for } x \geq a \\ 2q_0 \left[\frac{x}{a} + \left(\frac{x^2}{a^2} - 1 \right)^{1/2} \right] & \text{for } x \leq -a \\ 2q_0 \frac{x}{a} - p_0 \left(1 - \frac{x^2}{a^2} \right)^{1/2} & \text{for } |x| \leq a \end{cases}$$

The maximum normal and tangential stresses are p_0 and q_0 , respectively.

Contour and Variation of Stress

Graphs removed for copyright reasons.
See Figures 4.9 through 4.15 in [Suh 1986].

Crack Growth of Hertzian Crack

(soda-lime glass in air)

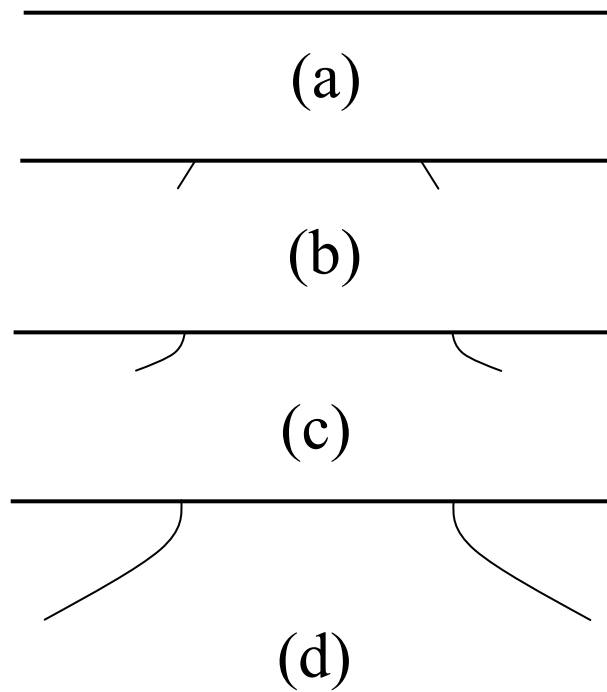


Figure 4.16

Surface Traces of Hertzian Cracks on Surface of Silicon

Photos removed for copyright reasons.
See Figure 4.18 in [Suh 1986].

Crack Patterns on Sod-lime Glass Produced by Sliding Tungsten Carbide Sphere

Photos removed for copyright reasons.
See Figure 4.17 in [Suh 1986].

“Star” Crack in Soda-Lime Glass produced by Conical Indenter

Photos removed for copyright reasons.
See Figure 4.19 in [Suh 1986].

Sequence of Crack Formation and Growth Events during Loading and Unloading

Photos removed for copyright reasons.
See Figure 4.20 in [Suh 1986].